Published in final edited form as:
Peptides. 2009 May ; 30(5): 849–854. doi:10.1016/j.peptides.2009.01.027.

Amyloid-beta peptide Aβp3-42 affects early aggregation of full-length Aβ1-42

Hiromi M. Sanders[*,a], **Robert Lust**[c], and **Jan K. Teller**[b]
Department of Physiology, East Carolina University Brody School of Medicine, Greenville, NC, 27834

Abstract

The major amyloid beta (Aβ) peptides found in the brain of familial and late onset Alzheimer's disease include the full-length Aβ1-42 and N-terminally truncated, pyroglutamylated peptides Aβp3-42 and Aβp11-42. The biophysical properties of Aβ1-42 have been extensively studied, yet little is known about the other modified peptides. We investigated the aggregation kinetics of brain-specific Aβ peptides to better understand their potential roles in plaque formation. Synthetic peptides were analyzed individually and in mixtures representing various ratios found in the brain. Spectrofluorometric analyses using Thioflavin-T showed that the aggregation of Aβ1-42 was faster compared to Aβp3-42; however, Aβp11-42 displayed similar kinetics. Surprisingly, mixtures of full-length Aβ1-42 and Aβp3-42 showed an initial delay in beta-sheet formation from both equimolar and non-equimolar samples. Electron microscopy of peptides individually and in mixtures further supported fluorescence data. These results indicate that Aβ-Aβ peptide interactions involving different forms may play a critical role in senile plaque formation and maintenance of the soluble Aβ pool in the brain.

Keywords

Alzheimer's disease; Amyloid-beta peptides; Aggregation; Pyroglutamate

1. Introduction

Protein aggregation is a pathological feature of many neurodegenerative diseases. Alzheimer's disease (AD), the most prevalent form of senile dementia, is characterized by extracellular deposits of amyloid-beta (Aβ) peptides forming the characteristic senile plaques [7]. Aβ is a 39 to 43 amino acid peptide derived through the proteolytic processing of the amyloid precursor protein (APP) [32]. Cleavage of this transmembrane protein by specific secretases, releases a family of Aβ peptides, which subsequently aggregate to form larger fibrillar structures ultimately developing into diffuse or compact senile plaques [32]. This process appears to be accelerated in both familial AD and Down's syndrome (DS). Familial AD is caused by

*Corresponding author: Hiromi M.Sanders, Columbia University Medical Center, Irving Cancer Research Center, 1130 St.Nicholas Ave., New York, NY 10032 Phone: 212-851-4756, Fax: 212-342-0484, hs2386@columbia.edu.
[a]Current address: Columbia University Medical Center, New York, NY 10032
[b]Current address: Dystonia Medical Research Foundation, Chicago, IL 60601
[c]Current address: East Carolina University Brody School of Medicine, Greenville, NC 27834

mutations in genes encoding either APP or presenilins 1 or 2, which participate in APP proteolytic processing among other genes [1,3–6,8,13,14,26,33]. Individuals with these mutations develop symptoms much earlier in life compared to late onset AD. In DS, increased expression of the APP gene as a result of trisomy 21, also leads to Alzheimer-like pathology early in life [21,32].

Senile plaques are composed primarily of a mixture of both 40 and 42 amino acid Aβ peptides. Full-length Aβ1-42 predominates in both AD and DS [7,18,22,36]. Numerous studies have shown that Aβ1-42 has a greater propensity to aggregate compared to the shorter counterpart, Aβ1-40 [2]. Analysis of the senile plaques as well as water-soluble Aβ has revealed a heterogeneous mixture of truncated, modified peptides along with full-length Aβ peptides [12,16,18,24,26,28,29,34]. Two N-terminally truncated peptides, Aβp3-42 and Aβp11-42, have their N-terminal glutamates cyclized. The two peptides are interesting in that both are found in plaques of AD and DS brains, and specifically in DS brain, are present in soluble form long before the appearance of insoluble plaques [24,25,36]. Despite difficulties in measuring these peptides in brain extracts, microgram levels of the modified peptides were found in both AD and DS brain [36]. For instance, the concentration of Aβp3-42 has been shown to increase as the disease progresses and in some cases may account up to 25% of the total Aβ load [10, 24]. Moreover, Aβp11-42 is specifically elevated in certain familial cases with presenilin mutations [26]. Due to structural modifications, both pyroglutamylated peptides are more resistant to peptidases, which may explain their dominance in senile plaques [28]. Furthermore, N-terminal truncation of Aβ peptides increases their hydrophobicity, which leads to increased propensity to aggregate compared to Aβ1-42 [19]. However, to date no exhaustive comparative analyses of the N-terminally truncated, pyroglutamylated peptides have been conducted.

In this study, we set out to compare the aggregation kinetics of synthetic full-length Aβ1-42, Aβp3-42, and Aβp11-42 peptides. We used Thioflavin-T (ThT) as an indicator of β-sheet formation to monitor peptide aggregation. Our results show that full-length Aβ1-42 forms β-sheets more readily compared to the N-terminally modified peptides. Yet unexpectedly, Aβp3-42 added to full-length Aβ1-42 at various ratios causes significant alterations in the propensity of full-length Aβ1-42 to aggregate specifically during the initial phases of aggregation.

2. Materials and methods

2.1. Chemicals and peptides

Synthetic Aβ peptides were purchased from AnaSpec (San Jose, CA): Aβ1-42 (Lot n.31475), Aβp3-42 (Lot n.29907), Aβp11-42 (Lot n.29903). HEPES free acid, Glycerol, and 2-mercaptoethanol were purchased from Sigma Aldrich (St.Louis, MO). TRIS, Acrylamide (Electrophoretic grade), Bis-acrylamide (Electrophoretic grade), Glycine, Tricine, Methanol (HPLC grade), Sodium Chloride, and Coomassie Brilliant Blue G-250 were purchased from Fisher Chemicals (Atlanta, GA). Sodium dodecyl sulphate (SDS) was purchased from Bio-Rad (Hercules, CA). 1,1,1,3,3,3-Hexafluoro-2-propanol (HFIP) and Thioflavin-T (ThT) were purchased from Sigma Aldrich (St.Louis, MO). Sodium phosphotungstate was purchased from Sigma (St.Louis, MO) and Formvar substrate-Nickel grids for Electron Microscopy were purchased from Ladd Research (Williston, VT).

2.2 Aβ sample preparation

One mL of cold 1,1,1,3,3,3-hexafluoro-2-propanol (HFIP) was added to 1mg of lyophilized peptide, for a final concentration of 1mg/mL. Aliquots of 100μL were stored in −80°C until needed. Before experiments, the required amounts of peptides in HFIP were aliquoted and vacufuged for 10 minutes. A mixture of 0.2% $NHOH_4$ and 100mM Hepes at a ratio of 1:9 was

added to solubilize dried peptides for approximately 5–10 minutes followed with 500mM Hepes and double-deionized H_2O. All solutions were prepared at physiological pH of 7.4. Aβ samples were constantly stirred throughout the experiments at 25°C.

2.3. Fluorometic analysis

Thioflavin-T was added to each Aβ sample to a final concentration of 20μM. Peptide aggregation was monitored by recording ThT fluorescence using the SPEX Fluoromax-3 spectrofluorometer (HORIBA Group, Edison, NJ). ThT excitation and emission wavelengths were 450nm and 485nm, respectively. Measurements were taken every 15 minutes for the first two hours and every hour thereafter up to 24 hours. Every effort was made to minimize exposure of samples to light to avoid degradation of ThT. All experiments were independently conducted a minimum of three times. Vehicle samples without peptide were prepared fresh for each assay conducted. Fluorescence readings from Aβ samples were corrected for background changes in fluorescence by subtracting values from vehicle preparations without peptide. Results are expressed as average fluorescence units with mean values ± SE of a minimum of three independent experiments. ANOVA followed by Fisher's Post-Hoc analysis was conducted on each sample for each individual time point. Statistical significance was achieved with p values less than 0.05.

2.4. Western Blot

Samples were analyzed for the presence of specific peptides and aggregates by Western blotting. Sample buffer without reducing agents such as SDS or β-mercaptoethanol was added to all samples. Non-denaturing tris-tricine gels were cast to separate monomeric from aggregate structures. Membranes were probed with antibody 4G8 (SENETEK, Napa, CA) specific for residues 17–24 of Aβ and antibody PC421 specific for Aβx-42. Membranes were also probed with antibodies AβN3(pE) and AβN11(pE) provided by T.C. Saido to identify pyroglutamylated species Aβp3-42 and Aβp11-42, respectively [28].

2.5. Electron microscopy

Peptide samples were prepared as described for the ThT experiments and aggregated at 25°C with constant agitation. Five to ten μL of sample preparation was added to carbon and Formvar-coated nickel grids for 3–5 minutes and blotted with filter paper. A 2% solution of sodium phosphotungstate at pH 7.0 was added immediately as the staining agent. After one minute the grid was quickly and completely dried with filter paper. Grids were analyzed using the FEI/Philips EM 208S transmission electron microscope. Two grids were treated for each sample analyzed. Multiple images were taken from each grid and images shown are representative peptide structures observed on the grids at the indicated times. Grids of the vehicle only were analyzed to discriminate between actual peptide and background.

3. Results

We prepared samples using synthetic Aβ peptides and analyzed the rate of aggregation by monitoring ThT fluorescence to compare the kinetics of aggregation of full-length Aβ1-42 and the N-terminally truncated, pyroglutamylated peptides Aβp3-42 and Aβp11-42. Individual peptide samples were prepared at final concentrations of 5μM. Small volumes were collected for the analysis of peptide aggregates by using Western blotting. As expected, membranes probed with the antibody 4G8 confirmed the presence and predominance of monomeric forms in each sample at the beginning of the assays (Fig.1A, B).

Inspection of the fluorometric data indicates that full-length Aβ1-42 aggregates similarly to Aβp11-42, yet much faster than Aβp3-42 (Fig.2). In repeated assays, 5μM Aβ1-42 and Aβp11-42 reached maximum ThT fluorescence between three to five hours, while contrary to

previous findings, aggregation of 5μM Aβp3-42 was much slower [12,27]. In fact, the time required to reach 50% of the maximum fluorescence intensity, the T_{50} value, for Aβ1-42 was just under three hours while Aβp3-42 reached half maximum many hours later (data not shown). However, Western blot analysis confirmed the presence of larger aggregates formed from all peptides at the end of the assays showing antibody labeling at the bottom of loading wells, suggesting the presence of larger aggregates (Fig.1C–E).

From individual fluorescence data, we hypothesized that preparing mixtures of the fastest and slowest aggregating peptides would result in intermediate kinetics. Since Aβ1-42 and Aβp3-42 aggregated the fastest and slowest respectively, we prepared various mixtures of the two peptides and measured ThT fluorescence over time. In our first mixture at 10μM, we observed lower fluorescence readings early (Fig.2), yet higher readings as aggregation continued which was expected due to the higher concentration of peptides [15]. However, fluorescence measurements did not reach that of Aβ1-42 alone until after it reached maximum fluorescence. Next, we prepared mixtures of the two peptides at a concentration of 2.5 μM each. Surprisingly, this peptide mixture aggregated in the same fashion as reported for 5μM Aβp3-42 alone (Fig. 2). Therefore, the data suggests that in equimolar mixtures at two different concentrations, Aβp3-42 delayed early aggregation of Aβ1-42. Again, Western blots confirmed the presence of both peptides at the beginning of the assay in monomeric form (Fig.1B). Samples collected at the end of the assay confirm the presence of peptide aggregates at the bottom of loading wells (Fig.1D, E), indicating the formation of larger homogeneous or heterogeneous aggregates similar to those seen in brain extracts [28].

To test whether the same effect could be reproduced at other peptide ratios, we prepared non-equimolar mixtures with final concentrations of 6μM. A five to one micromolar ratio of full-length to Aβp3-42 aggregated similarly to 6μM Aβ1-42 alone (Fig.3). However, a two to one ratio displayed the same delay in aggregation as observed earlier in equimolar mixtures. A final equimolar mixture of 3μM Aβ1-42 and 3μM Aβp3-42 reproduced that of Aβp3-42 aggregation at 6μM alone (Fig.3). It appears that as more Aβp3-42 was added with Aβ1-42, a reduction in ThT incorporation occurred early, indicative of a delay in beta-sheet formation during initial stages of aggregation. In addition, T_{50} values for the peptide mixture at a ratio of 2:1 were approximately 4.8 hours, which was significantly higher than the T_{50} of full-length Aβ1-42 alone, which was less than two hours (data not shown). Therefore, these results further supports the notion that the N-terminally truncated, modified peptide Aβp3-42 exerts an inhibitory affect on aggregation of full-length Aβ1-42, specifically during early phases.

According to our data, the greatest difference in aggregation occurred two to four hours into the fluorometric assay. This difference was observed for the full-length Aβ1-42 and Aβp3-42 peptides individually as well as in mixtures of the two peptides. To observe the peptide aggregates, we analysed samples collected after two and four hours using electron microscopy (EM) and found heterogeneous structures present in most samples. Images of 6μM Aβ1-42 displayed mostly immature fibrillar structures similar to those described previously (Fig.4A, B) [31]. The criteria included the occurrence of flexions and curved fibers. We did observe shorter, curly fibers from the two hour time point; yet the majority were longer, fibrillar structures with multistrand organization [31]. Images of 6μM Aβp3-42 showed mostly short fibers aligned side-by-side forming small bundles (Fig.4C, D). Bundles of short, aligned fibers and mostly curly fibers loosely gathered were also present (Fig.4D). Although EM is not quantitative, images of Aβp3-42 forming immature fibers were difficult to locate when compared to full-length Aβ1-42, which was consistent with our fluorescence data.

EM images from mixtures of 3μM Aβ1-42 and 3μM Aβp3-42 were fairly similar to Aβp3-42 images captured at both time points (Fig.4 E, F); mostly patches of smaller bundles consisting of short, straight and curly fibers. Images taken after two hours of the 4μM Aβ1-42 and 2μM

Aβp3-42 mixture showed a few patches of longer fibers forming a net-like structure surrounded by globular chains as previously reported (Fig.4 G) [27, 38]. After four hours of aggregation, there appeared an abundance of immature fibrillar structures similar to Aβ1-42 with structures previously observed including the flexions, curved fibers, and multistrand twistings (Fig.4H).

4. Discussion

Alzheimer's disease develops over many years before any symptoms appear. The exact pathogenic mechanisms of this illness have not been elucidated. However, since the discovery and isolation of Aβ peptides as the major component of senile plaques found in AD brain, the focus has been centered on these peptides [7]. In particular, the accumulation of the heterogeneous peptide isoforms may be considered causative in the development of the disease [1,3–9,13,14,20,25,26,33]. Due to its prevalence in senile plaques and unusual propensity to aggregate, full length Aβ1-42 has been extensively studied [7,22,23]. Less attention has been devoted to the truncated, modified peptides also abundant in the brain.

Since truncated, pyroglutamylated Aβ peptides aggregate more readily, are more resistant to proteases, and are prevalent in AD and DS brain, we specifically included these peptides in our studies [16,19,24,28,29]. The aggregation of non-modified peptides may precede the formation of cyclized glutamate residues, however the observation from Teller et al. that modified peptides are found in abundance in diffuse plaques strongly suggests that the modification indeed occurs prior to plaque formation [25,30,36]. Our goals were to study the aggregation of synthetic, brain-specific, N-terminally truncated, modified peptides and compare to that of full-length Aβ1-42. As the levels of the pyroglutamylated peptides are elevated in the brain of AD and DS individuals and that senile plaque are heterogeneous in nature, we also decided to visually analyze mixtures representing peptide ratios found in the brain.

We report here that full-length Aβ1-42 aggregates faster than the specific N-terminally truncated, pyroglutamylated Aβp3-42 isoform; yet the rate of aggregation of Aβp11-42 is quite similar, if not the same. This is not consistent with previous reports indicating that N-terminally truncated, pyroglutamylated peptides aggregate faster than full-length Aβ peptides [12,19, 27]. It is important to note that in Pike *et al.'s* study, the modified peptides were not analyzed [19]. The cyclization of glutamate residues, which alters the peptide structure, may affect the aggregation propensity. He *et al.* and Russo *et al*. reported enhanced aggregation of the pyroglutamylated peptides compared to the full-length peptide [12,27]. Their studies differ significantly from our study since they used shorter, 28 and 40 amino acid long Aβ peptides, used much higher concentrations of peptides, and analyzed peptides only after three days of incubation at 37° C. Other studies using full-length Aβ1-42 and Aβp3-42 have reported beta-pleated sheets present in both fresh and aged peptides, however beta-sheet formation through time was not analyzed [35]. Furthermore, our study shows a delay in the early phases of aggregation, not fibrillization. The fluorescence data of Aβp3-42 as well as EM images shows that at the early time points, the peptide gradually makes the transition from smaller aggregates into fibrillar structures, leading us to speculate that the seeding or nucleation phase may be slower. However, fluorescence measurements of Aβp3-42 aggregation after ten hours did show a continuous rise in ThT fluorescence (data not shown), indicating both aggregation and fibrillization had occurred. Western blot analyses of Aβp3-42 show larger structures at the end of aggregation assays from samples analyzed many hours later, further suggesting that both aggregation and fibrillization had occurred.

Reasons for this discrepancy may be that binding of ThT is altered while in the presence of Aβp3-42 due to both N-terminal truncation and peptide structure. In contrast, fluorometric analysis showed that ThT bound well to the Aβp11-42 isoform, dismissing this idea. Yet the

difference between the isoforms is the overall length of the peptides and their hydrophobicity. Greater hydrophobicity of Aβp11-42 due to an increased number of charges removed would explain its higher propensity to aggregate, despite modification. The Aβp3-42, in contrast, is perhaps unable to form stable structures compared to other peptides. It is possible that larger structures were being formed but were unstable and as a result the formation of fibrils, where ThT could intercalate was impaired. Nevertheless, there were plenty of variables that could have accounted for the differences in published data such as solutions used, pH values, total concentrations, temperature, etc. These aspects could have caused differences by either accelerating or impeding the aggregating process.

At three separate equimolar mixtures of full-length Aβ1-42 and Aβp3-42, we found that aggregation was altered during the initial hours. Both 2.5μM and 5.0μM per peptide mixtures showed a delay in early aggregation when compared to Aβ1-42 alone, while 3μM per peptide mixtures altered aggregation throughout the entire time course. One could speculate the lower fluorescence readings indicative of delays in aggregation, could have been the result of lower Aβp3-42 concentrations in the mixed samples. However, this is not seen in those mixtures with 2.5μM and specifically 5.0μM per peptide. With equimolar ratios, it is clearly observed that the delay in aggregation remains within the initial hours of aggregation assays. Yet, we were compelled to conduct nonequimolar aggregation assays to not only, mimic those ratios found in the diseased brain but to also compare individual peptide assays to that of mixed samples with the same total concentration. In this way, proper analyses on the aggregation of mixed samples could be made. Thus, it appears that Aβp3-42 had an affect on the initial process of aggregate formation while in the presence of Aβ1-42, which was not surprising given the aggregation of Aβp3-42 alone. From the EM images, it was clear that the presence of longer extending fibers and fiber bundles, characteristic of Aβ1-42, was increased as the Aβp3-42 amount decreased. As more Aβp3-42 was added to full-length Aβ1-42 however, the appearance of compact fibrillar structures became much more difficult to discern compared to ratios favoring Aβ1-42. This latter observation further supported the fluorescence data in suggesting an inhibitory role of Aβp3-42 on Aβ1-42 aggregation.

The inhibitory role of Aβp3-42 in the aggregation of full-length Aβ1-42 has not been reported. A possible mechanism may involve a disruption in nucleation or the seeding process by Aβp3-42, which inhibits the early phase of Aβ1-42 aggregation. This disruption may be the result of the structural modification present in Aβp3-42, which may obstruct peptide interaction. Another mechanism may involve Aβp3-42 forming unstable aggregates, which may collapse and potentially affect other larger aggregates. The deposition of Aβp3-42 early in the brain may constitute a mechanism to prevent or disrupt the deleterious accumulation of Aβ peptides. This may appear to contradict the recent studies by Schilling et al. (2006), in which the authors demonstrated that N-terminal truncation and in particular, pyroglutamyl formation may lead to increased amyloidogenicity [30]. In our fluorescence data, one could also speculate that Aβp3-42 may increase aggregation upon interaction with Aβ1-42. Unfortunately, we did not focus on the fibrillization phases but instead focused our efforts on the initial phases of aggregation. However, it is of note that as reported by both Zou et al. and Yan et al., the Aβ1-40 had similar inhibitory effects on the aggregation of full-length Aβ1-42 as the modified peptide Aβp3-42 had on Aβ1-42 in our study: in the presence of Aβ1-40, transition of Aβ1-42 to beta-sheet was reduced as shown by circular dichroism spectroscopy, electron microscopy and nuclear magnetic resonance [37,39]. Yan et al. conducted an elegant experiment showing monomeric Aβ1-42 species decreasing after only 3hours of aggregation on Western blots [37]. When Aβ1-40 monomers were introduced with Aβ1-42, monomeric forms of Aβ1-42 remained much longer indicative of an inhibition of Aβ1-42 aggregation by Aβ1-40. Hasegawa et al. kept constant Aβ1-42 concentrations while changing Aβ1-40 and as well as kept Aβ1-40 constant while Aβ1-42 levels changed [11]. Although their focus was on the interaction of different species of peptides, they reported a similar inhibitory effect

characterized by an interruption in Aβ1-42 conformation changes during the nucleation or initial phases of aggregation. We believe our studies would mimic those of Hasegawa and Yan et al. when conducted in a similar fashion [11,37].

One must take into consideration that the peptides used in this and numerous other studies were synthetic, which limits the interpretation of biochemical and biophysical results in the context of AD development and progression. As shown by Meyer-Luehmann et al., brain-derived Aβ peptide mixtures differed considerably from synthetic mixtures in terms of their capacity to induce amyloid deposition in the rodent brain [17]. Nonetheless, our data provides further proof that the role N-terminally truncated, pyroglutamylated peptides have the potential to play a critical role in the development and progression of Alzhiemer's disease.

Acknowledgements

We would like to thank Dr.Michael Dykstra from North Carolina State University College of Veterinary Medicine Laboratory for Advanced Electron and Light Optical Methods (LAELOM) for his gracious help in obtaining EM images, Dr.Robert Carroll and Dr.Rebecca Nolan-Harris for their help with critical thinking and analysis and Dr.Gregory Harris for technical assistance. This work was supported by the NINDS and the John and Harriet Wooten Alzheimer's Disease Research Fund.

References

1. Borchelt DR, Thinakaran G, Eckman CB, Lee MK, Davenport F, Ratovitsky T, et al. Familial Alzheimer's disease-linked presenilin 1 variants elevate Abeta1-42/1-40 ratio in vitro and in vivo. Neuron 1996;17:1005–1013. [PubMed: 8938131]
2. Burdick D, Soreghan B, Kwon M, Kosmoski J, Knauer M, Henschen A, et al. Assembly and aggregation properties of synthetic Alzheimer's A4/beta amyloid peptide analogs. J Biol Chem 1992;267:546–554. [PubMed: 1730616]
3. Cai XD, Golde TE, Younkin SG. Release of excess amyloid beta protein from a mutant amyloid beta protein precursor. Science 1993;259:514–516. [PubMed: 8424174]
4. Citron M, Oltersdorf T, Haass C, McConlogue L, Hung AY, Seubert P, et al. Mutation of the beta-amyloid precursor protein in familial Alzheimer's disease increases beta-protein production. Nature 1992;360:672–674. [PubMed: 1465129]
5. Citron M, Westaway D, Xia W, Carlson G, Diehl T, Levesque G, et al. Mutant presenilins of Alzheimer's disease increase production of 42-residue amyloid beta-protein in both transfected cells and transgenic mice. Nat Med 1997;3:67–72. [PubMed: 8986743]
6. Duff K, Eckman C, Zehr C, Yu X, Prada CM, Perez-tur J, et al. Increased amyloid-beta42(43) in brains of mice expressing mutant presenilin 1. Nature 1996;383:710–713. [PubMed: 8878479]
7. Glenner GG, Wong CW. Alzheimer's disease and Down's syndrome: sharing of a unique cerebrovascular amyloid fibril protein. Biochem Biophys Res Commun 1984;122:1131–1135. [PubMed: 6236805]
8. Hardy J. Amyloid, the presenilins and Alzheimer's disease. Trends Neurosci 1997;20:154–159. [PubMed: 9106355]
9. Hardy J, Duff K, Hardy KG, Perez-Tur J, Hutton M. Genetic dissection of Alzheimer's disease and related dementias: amyloid and its relationship to tau. Nat Neurosci 1998;1:355–358. [PubMed: 10196523]
10. Harigaya Y, Saido TC, Eckman CB, Prada CM, Shoji M, Younkin SG. Amyloid beta protein starting pyroglutamate at position 3 is a major component of the amyloid deposits in the Alzheimer's disease brain. Biochem Biophys Res Commun 2000;276:422–427. [PubMed: 11027491]
11. Hasegawa K, Yamaguchi I, Omata S, Gejyo F, Naiki H. Interaction between A beta(1-42) and A beta (1-40) in Alzheimer's beta-amyloid fibril formation in vitro. Biochemistry 1999;38:15514–15521. [PubMed: 10569934]
12. He W, Barrow CJ. The A beta 3-pyroglutamyl and 11-pyroglutamyl peptides found in senile plaque have greater beta-sheet forming and aggregation propensities in vitro than full-length A beta. Biochemistry 1999;38:10871–10877. [PubMed: 10451383]

13. Holcomb L, Gordon MN, McGowan E, Yu X, Benkovic S, Jantzen P, et al. Accelerated Alzheimer-type phenotype in transgenic mice carrying both mutant amyloid precursor protein and presenilin 1 transgenes. Nat Med 1998;4:97–100. [PubMed: 9427614]

14. Hsiao K, Chapman P, Nilsen S, Eckman C, Harigaya Y, Younkin S, et al. Correlative memory deficits, Abeta elevation, and amyloid plaques in transgenic mice. Science 1996;274:99–102. [PubMed: 8810256]

15. Jarrett JT, Lansbury PT Jr. Seeding "one-dimensional crystallization" of amyloid: a pathogenic mechanism in Alzheimer's disease and scrapie? Cell 1993;73:1055–1058. [PubMed: 8513491]

16. Kuo YM, Emmerling MR, Woods AS, Cotter RJ, Roher AE. Isolation, chemical characterization, and quantitation of A beta 3-pyroglutamyl peptide from neuritic plaques and vascular amyloid deposits. Biochem Biophys Res Commun 1997;237:188–191. [PubMed: 9266855]

17. Meyer-Luehmann M, Coomaraswamy J, Bolmont T, Kaeser S, Schaefer C, Kilger E, et al. Exogenous induction of cerebral beta-amyloidogenesis is governed by agent and host. Science 2006;313:1781–1784. [PubMed: 16990547]

18. Naslund J, Schierhorn A, Hellman U, Lannfelt L, Roses AD, Tjernberg LO, et al. Relative abundance of Alzheimer A beta amyloid peptide variants in Alzheimer disease and normal aging. Proc Natl Acad Sci U S A 1994;91:8378–8382. [PubMed: 8078890]

19. Pike CJ, Overman MJ, Cotman CW. Amino-terminal deletions enhance aggregation of beta-amyloid peptides in vitro. J Biol Chem 1995;270:23895–23898. [PubMed: 7592576]

20. Prasher VP, Farrer MJ, Kessling AM, Fisher EM, West RJ, Barber PC, et al. Molecular mapping of Alzheimer-type dementia in Down's syndrome. Ann Neurol 1998;43:380–383. [PubMed: 9506555]

21. Reeves RH. Down's syndrome. A complicated genetic insult. Lancet 2001;358:S23. [PubMed: 11784572]

22. Roher AE, Lowenson JD, Clarke S, Wolkow C, Wang R, Cotter RJ, et al. Structural alterations in the peptide backbone of beta-amyloid core protein may account for its deposition and stability in Alzheimer's disease. J Biol Chem 1993;268:3072–3083. [PubMed: 8428986]

23. Roher AE, Lowenson JD, Clarke S, Woods AS, Cotter RJ, Gowing E, et al. beta-Amyloid-(1-42) is a major component of cerebrovascular amyloid deposits: implications for the pathology of Alzheimer disease. Proc Natl Acad Sci U S A 1993;90:10836–10840. [PubMed: 8248178]

24. Russo C, Saido TC, DeBusk LM, Tabaton M, Gambetti P, Teller JK. Heterogeneity of water-soluble amyloid beta-peptide in Alzheimer's disease and Down's syndrome brains. FEBS Lett 1997;409:411–416. [PubMed: 9224700]

25. Russo C, Salis S, Dolcini V, Venezia V, Song XH, Teller JK, et al. Amino-terminal modification and tyrosine phosphorylation of [corrected] carboxy-terminal fragments of the amyloid precursor protein in Alzheimer's disease and Down's syndrome brain. Neurobiol Dis 2001;8:173–180. [PubMed: 11162251]

26. Russo C, Schettini G, Saido TC, Hulette C, Lippa C, Lannfelt L, et al. Presenilin-1 mutations in Alzheimer's disease. Nature 2000;405:531–532. [PubMed: 10850703]

27. Russo C, Violani E, Salis S, Venezia V, Dolcini V, Damonte G, et al. Pyroglutamate-modified amyloid beta-peptides--AbetaN3(pE)--strongly affect cultured neuron and astrocyte survival. J Neurochem 2002;82:1480–1489. [PubMed: 12354296]

28. Saido TC, Iwatsubo T, Mann DM, Shimada H, Ihara Y, Kawashima S. Dominant and differential deposition of distinct beta-amyloid peptide species, A beta N3(pE), in senile plaques. Neuron 1995;14:457–466. [PubMed: 7857653]

29. Saido TC, Yamao-Harigaya W, Iwatsubo T, Kawashima S. Amino- and carboxyl-terminal heterogeneity of beta-amyloid peptides deposited in human brain. Neurosci Lett 1996;215:173–176. [PubMed: 8899741]

30. Schilling S, Lauber T, Schaupp M, Manhart S, Scheel E, Bohm G, et al. On the seeding and oligomerization of pGlu-amyloid peptides (in vitro). Biochemistry 2006;45:12393–12399. [PubMed: 17029395]

31. Seilheimer B, Bohrmann B, Bondolfi L, Muller F, Stuber D, Dobeli H. The toxicity of the Alzheimer's beta-amyloid peptide correlates with a distinct fiber morphology. J Struct Biol 1997;119:59–71. [PubMed: 9216088]

32. Selkoe DJ, Podlisny MB. Deciphering the genetic basis of Alzheimer's disease. Annu Rev Genomics Hum Genet 2002;3:67–99. [PubMed: 12142353]

33. Suzuki N, Cheung TT, Cai XD, Odaka A, Otvos L Jr, Eckman C, et al. An increased percentage of long amyloid beta protein secreted by familial amyloid beta protein precursor (beta APP717) mutants. Science 1994;264:1336–1340. [PubMed: 8191290]

34. Tekirian TL. Commentary: Abeta N- Terminal Isoforms: Critical contributors in the course of AD pathophysiology. J Alzheimers Dis 2001;3:241–248. [PubMed: 12214065]

35. Tekirian TL, Yang AY, Glabe C, Geddes JW. Toxicity of pyroglutaminated amyloid beta-peptides 3(pE)-40 and -42 is similar to that of A beta1-40 and -42. J Neurochem 1999;73:1584–1589. [PubMed: 10501204]

36. Teller JK, Russo C, DeBusk LM, Angelini G, Zaccheo D, Dagna-Bricarelli F, et al. Presence of soluble amyloid beta-peptide precedes amyloid plaque formation in Down's syndrome. Nat Med 1996;2:93–95. [PubMed: 8564851]

37. Yan Y, Wang C. Abeta40 protects non-toxic Abeta42 monomer from aggregation. J Mol Biol 2007;369:909–916. [PubMed: 17481654]

38. Yoshiike Y, Chui DH, Akagi T, Tanaka N, Takashima A. Specific compositions of amyloid-beta peptides as the determinant of toxic beta-aggregation. J Biol Chem 2003;278:23648–23655. [PubMed: 12716908]

39. Zou K, Kim D, Kakio A, Byun K, Gong JS, Kim J, et al. Amyloid beta-protein (Abeta)1-40 protects neurons from damage induced by Abeta1-42 in culture and in rat brain. J Neurochem 2003;87:609–619. [PubMed: 14535944]

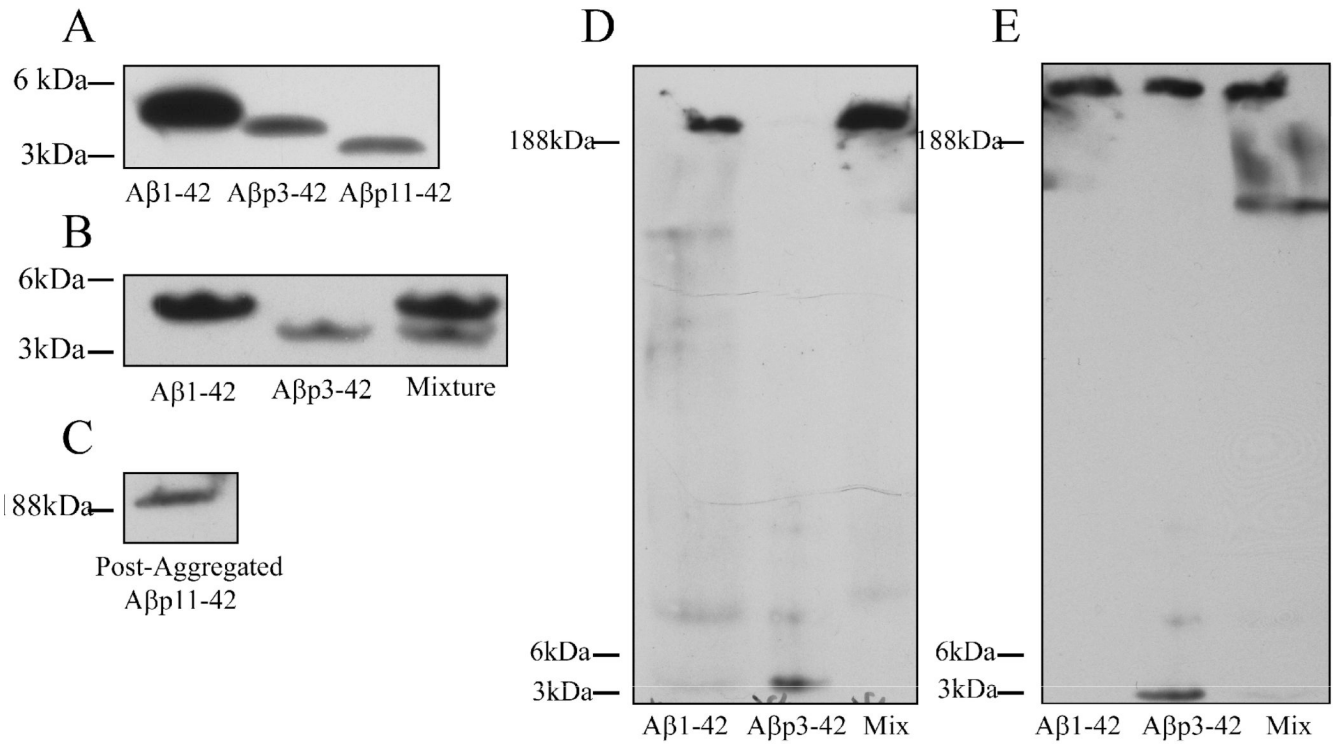

Figure 1.

Western blots confirm the presence of all peptides at the beginning of aggregation assays and that peptides were not degraded during aggregation. Western blots probed with antibody 4G8 show primarily monomeric peptides at the beginning of the assay; 4.5kDa Aβ1-42, 4.3kDa Aβp3-42, and 3.3kDa Aβp11-42 (A) as well as in samples of mixtures (B). (C) Depicts the aggregated form of Aβp11-42 peptide at the end of aggregation probed with the antibody AβN11(pE). (D) Western blot probed with 4G8 of peptides Aβ1-42 and Aβp3-42 at the end of aggregation assays, show the presence of larger aggregates. (E) Shows the same membrane reprobed with antibody AβN3(pE) to confirm the presence of both peptides in the mixture sample.

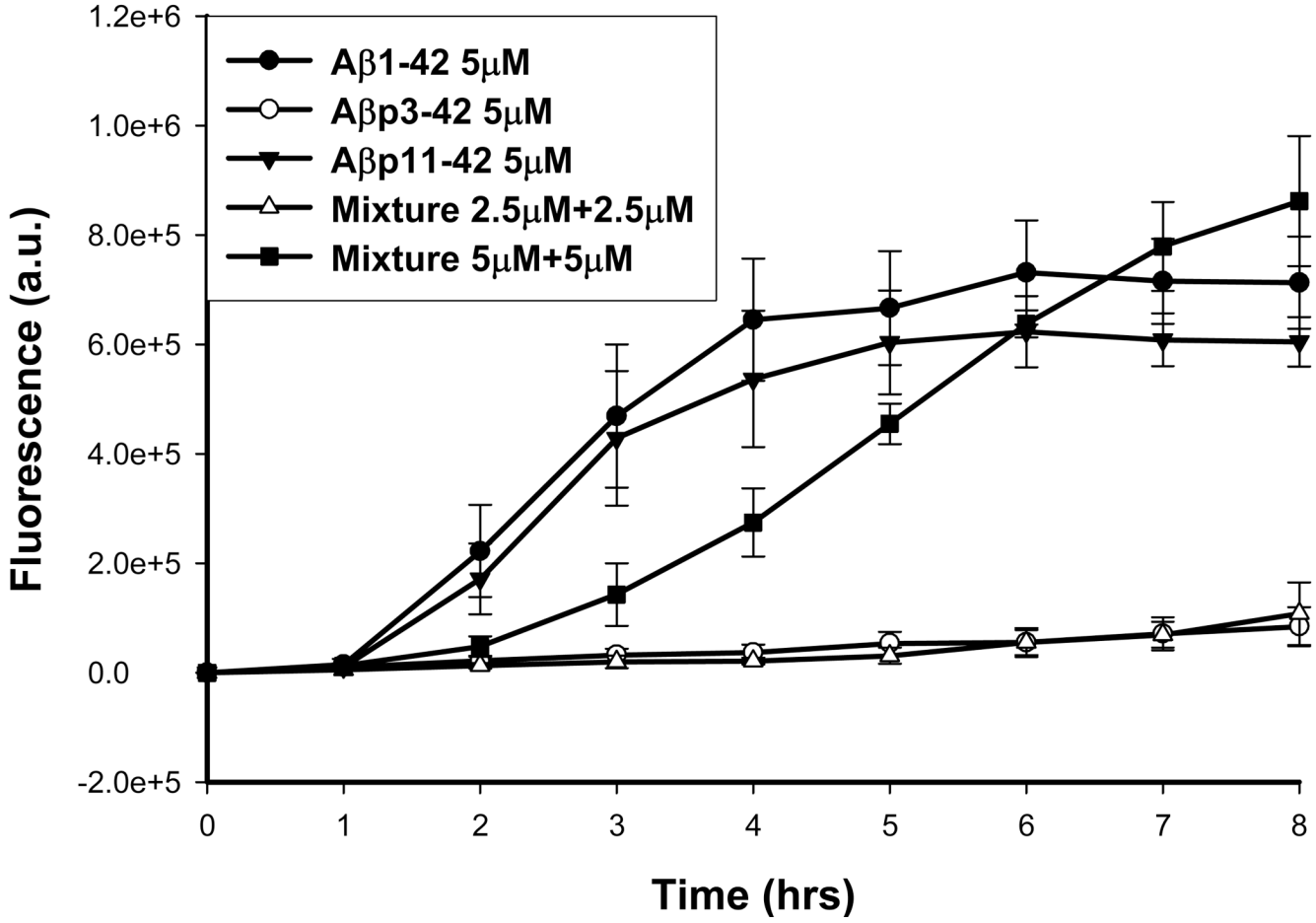

Figure 2.

Aβ1-42 and Aβp11-42 aggregate readily while Aβp3-42 forms larger aggregates very slowly. Equimolar mixtures of full-length Aβ1-42 with Aβp3-42 delay initial aggregation, compared to Aβ1-42 alone. Aggregation of synthetic peptides was measured using ThT fluorescence as an indicator of β-sheet formation at concentrations of 5μM for the first eight hours: (●) full-length Aβ1-42, (○) Aβp3-42, and (▼) Aβp11-42. Equimolar ratios of Aβ1-42 to Aβp3-42 were prepared to study aggregation over time. Mixtures of Aβ1-42 to Aβp3-42 include: 5μM+5μM (■) and 2.5μM+2.5μM (Δ). Results are expressed as average fluorescence units with mean values ±SE of a minimum of three independent experiments. ANOVA followed by Fisher's Post-Hoc analysis was conducted on each sample for each individual time point. Statistical significance was achieved with p values less than 0.05.

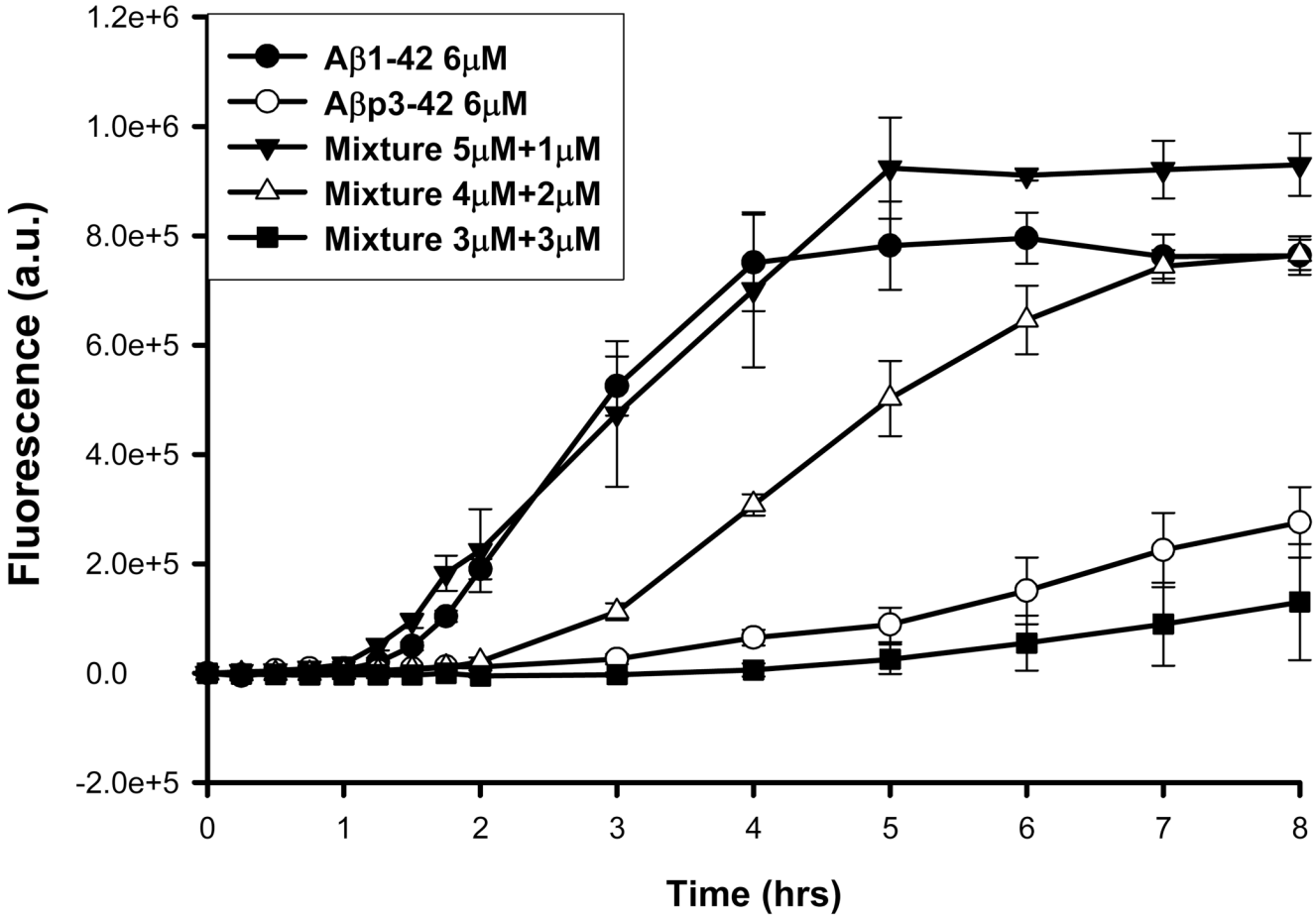

Figure 3.

Aβp3-42 delays initial aggregation of Aβ1-42 in non-equimolar mixtures. Various ratios of Aβ1-42 to Aβp3-42 were prepared to study aggregation over time. Individual peptides were at a concentration of 6μM: (●)Aβ1-42 and (○)Aβp3-42. Peptide mixtures of Aβ1-42 to Aβp3-42 include: 5μM+1μM (▼), 4μM+2μM (Δ), and 3μM+3μM (■). Results are expressed as average fluorescence units with mean values ± SE of a minimum of three independent experiments. ANOVA followed by Fisher's Post-Hoc analysis was conducted on each sample for each individual time point. Statistical significance was achieved with p values less than 0.05.

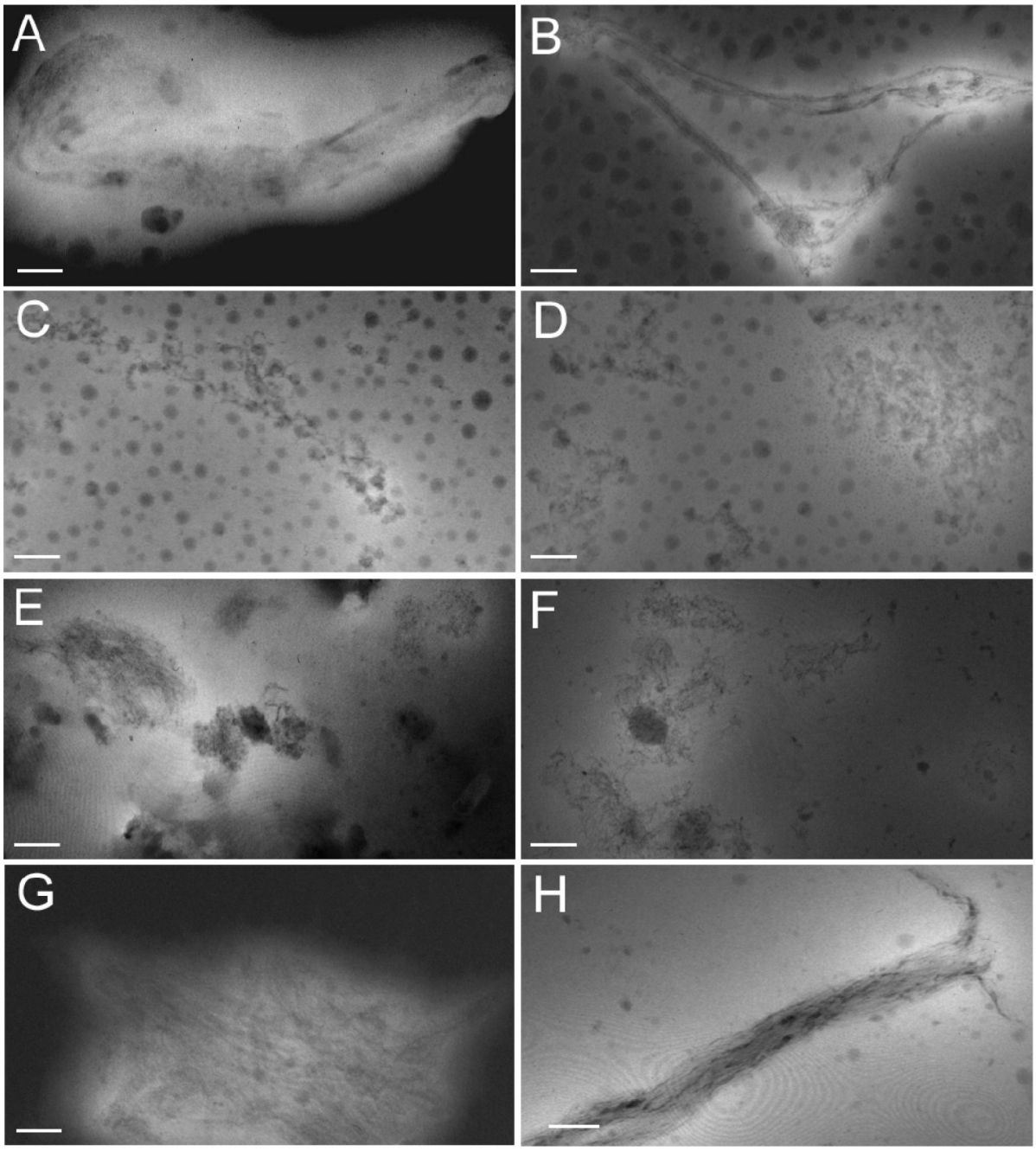

Figure 4.

Electron micrographs of Aβ1-42 and Aβp3-42 peptides aggregated individually (6μM) and in mixtures for two and four hours. After incubation, 5μl of each sample was prepared for electron microscopy as described. (A) Aβ1-42 aggregated for two hours showing curved, fibrillar structures. (B) Aβ1-42 after four hours of aggregation showing immature fibers consisting of flexions and curved fibers and the appearance of multistrand organization. (C) Aβp3-42 aggregated for two hours mostly contain closely gathered short and curly fibers. (D) Aβp3-42 image after four hours of aggregation was similar to the structures at the earlier time point. (E, F) Images of mixtures involving 3μM full-length Aβ1-42 and Aβp3-42 from both time points consisted mainly of small bundles of shorter, curly fibers, and longer, aligned fibers. (G)

Peptide mixture involving 4μM Aβ1-42 and 2μM Aβp3-42 consisted of bundles of aligned fibers after two hours of aggregation. (H) Images captured after four hours show the immature fibrillar structures with the flexions, curved fibers, and multistrand organization with occasional twisting similar to full-length Aβ1-42 alone. Magnification was 112,000; scale bars are 100μm.